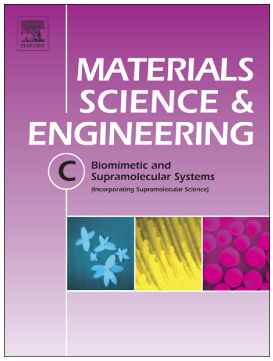


# β-pyrophosphate: A potential biomaterial for dental applications

A.D. Anastasiou, S. Strafford, O. Posada-Estefan, C.L. Thomson, S.A. Hussaein, T.J. Edwards, M. Malinowski, N. Hondow, N.K. Metzger, C.T.A. Brown, M.N. Routledge, A.P. Brown, M.S. Duggal, A. Jha

PII: S0928-4931(16)31912-9
DOI: doi: 10.1016/j.msec.2017.02.116
Reference: MSC 7450

To appear in: *Materials Science & Engineering C*

Received date: 25 October 2016
Revised date: 9 December 2016
Accepted date: 21 February 2017

Please cite this article as: A.D. Anastasiou, S. Strafford, O. Posada-Estefan, C.L. Thomson, S.A. Hussaein, T.J. Edwards, M. Malinowski, N. Hondow, N.K. Metzger, C.T.A. Brown, M.N. Routledge, A.P. Brown, M.S. Duggal, A. Jha , β-pyrophosphate: A potential biomaterial for dental applications. The address for the corresponding author was captured as affiliation for all authors. Please check if appropriate. Msc(2017), doi: 10.1016/j.msec.2017.02.116

# β-pyrophosphate; a potential biomaterial for dental applications.

A.D. Anastasiou[a], S. Strafford[b], O. Posada-Estefan[c], C.L. Thomson[d], S.A. Hussaein[d,e], T.J. Edwards[d], M. Malinowski[b], N. Hondow[a], N.K. Metzger[d], C.T.A. Brown[d], M.N. Routledge[c], A.P. Brown[a], M.S. Duggal[b], A. Jha[a]

[a] *School of Chemical and Process Engineering, University of Leeds, Leeds LS2 9JT, UK*

[b] *Leeds Dental School, Worsley Building, University of Leeds, Leeds LS2 9JT, UK*

[c] *Leeds Institute of Cardiovascular and Metabolic Medicine, Faculty of Medicine and Health, University of Leeds, LS2 9JT, UK*

[d] *SUPA, School of Physics and Astronomy, University of St Andrews, North Haugh, St Andrews, Fife, KY16 9SS, U.K.*

[e] *Cambridge Graphene Centre, Engineering Department, University of Cambridge, 9, JJ Thomson Avenue, Cambridge, CB3 0FA, UK*

**Corresponding Author:** Dr. Antonios D. Anastasiou

**Email:** a.anastasiou@leeds.ac.uk



**October 2016**

**Abstract**

Tooth hypersensitivity is a growing problem affecting both the young and ageing population worldwide. Since an effective and permanent solution is not yet available, we propose a new methodology for the restoration of dental enamel using femtosecond lasers and novel calcium phosphate biomaterials. During this procedure the irradiated mineral transforms into a densified layer of acid resistant iron doped β-pyrophosphate, bonded with the surface of eroded enamel. Our aim therefore is to evaluate this densified mineral as a potential replacement material for dental hard tissue. To this end, we have tested the hardness of β-pyrophosphate pellets (sintered at 1000 $^{o}$C) and its mineral precursor (brushite), the wear rate during simulated tooth-brushing trials and the cytocompatibility of these minerals in powder form. It was found that the hardness of the β-pyrophosphate pellets is comparable with that of dental enamel and significantly higher than dentine while, the brushing trials prove that the wear rate of β-pyrophosphate is much slower than that of natural enamel. Finally, cytotoxicity and genotoxicity tests suggest that iron doped β-pyrophosphate is cytocompatible and therefore could be used in dental applications. Taken together and with the previously reported results on laser irradiation of these materials we conclude that iron doped β-pyrophosphate may be a promising material for restoring acid eroded and worn enamel.

**Keywords**: calcium phosphate, enamel restoration, dental biomaterials, sintering, iron doping

## 1. Introduction

In dentistry tooth hypersensitivity is now considered as a growing problem affecting both the young and ageing populations worldwide. Surveys concerning the prevalence and distribution of the disease suggest that almost 10-15% of the general population suffer from tooth hypersensitivity (Smith and Grande, 2015). This percentage is expected to dramatically increase in future as advances in dental care result in more people retaining their natural teeth for longer (and consequently providing more opportunity for problems associated with enamel erosion). Literature suggests that the investigation of this condition started almost one century ago (e.g. (Croisier and Jérôme, 2013)) however, the exact mechanism that causes tooth hypersensitivity is not yet clear. What is certain is that the aetiology of the disease is linked with exposure of the dentine tubule system (lesion localisation) and this is the result of enamel loss. One suggested pathway to hypersensitivity occurs when dentine is stimulated with a hot or cold liquid; fluid flow in the exposed tubules triggers a mechanoreceptor response of the fibre nerves causing pain to the patients (Panseri et al., 2012). The quality of life for those affected by chronic dentinal hypersensitivity is markedly compromised as long term relief for pain is yet to be achieved.

The basic treatment strategies so far include; a) dentin blocking agents that occlude the exposed tubules (e.g. sodium chloride, hydroxyapatite based tooth pastes etc.) and b) desensitisation agents that reduce nerve sensitivity (Gillam et al., 2011). However, for cases with localised moderate or severe dental hypersensitivity immediate and long term relief is required and a number of additional restorative approaches may be followed. So far, various materials have been tested for enamel restoration. The acrylic resin is the most widely used. Usually, these products consist of a liquid and a powder; the powder contains beads of polymethyl – methacrylate and a chemical initiator (which may be a peroxide). The

liquid phase consists of methylmethacryalte monomer and a chemical activator. Generally, acrylic resins are less prone to erosion compared to other synthetic dental materials (e.g. silicates) because they have low solubility over a wide range of pH values (McCabe and Walls, 2013). Such polymeric materials suffer from significant disadvantages which demand regular intervention; acrylic materials are particularly sensitive to volumetric shrinkage against the hydroxyapatite present in dental enamel. Volume reductions up to 6% have been observed (Kleverlaan and Feilzer, 2005) and the resulting voids become active fillers for bacterial colonisation. Moreover, the lower compressive strength and hardness of resins compared to the natural mineral of teeth, result in poor durability especially during the application of abrasive forces (Yan et al., 2009). An effort to overcome these disadvantages led to the development of a new group of composite restorative materials. These consist of a resin phase and a reinforcing filler. Even though the mechanical properties are improved compared to acrylic resins, composites still do not reach the performance levels of dental enamel or dentine (McCabe and Walls, 2013). The substandard properties of current restorative materials is an important factor for the failure of enamel restoration in the long term and for the lack of a permanent solution to tooth hypersensitivity. On the other hand, solutions such as the use of commercial toothpastes containing nanoparticles (that occlude exposed dentine tubules) only provide temporary symptomatic relief as the pain returns when use of the product is stopped.

By recognising the outstanding issues of the current restorative materials we offer a radically new approach that utilises materials chemically similar to natural enamel. In our approach we have achieved the occlusion of the exposed dentine using femtosecond pulsed lasers and calcium phosphate based materials which match the thermal expansion coefficient and the mechanical properties of enamel and dentine. As depicted in **Fig. 1** the

proposed strategy can be described in three steps; **a**) cleaning and drying of the tooth surface; **b**) use of a microfluidic based delivery system to apply fresh calcium phosphate biomaterial on a defective area of a tooth to produce a thin, loosely adherent film (<30 μm); **c**) irradiation of the film with a femtosecond pulsed laser to densify the coating and promote bonding with the underlying tooth surface. If the proposed treatment is applied before complete loss of dental enamel and the exposure of dentine tubules, it could be a perfect procedure not only for the treatment but also for the prevention of tooth hypersensitivity.

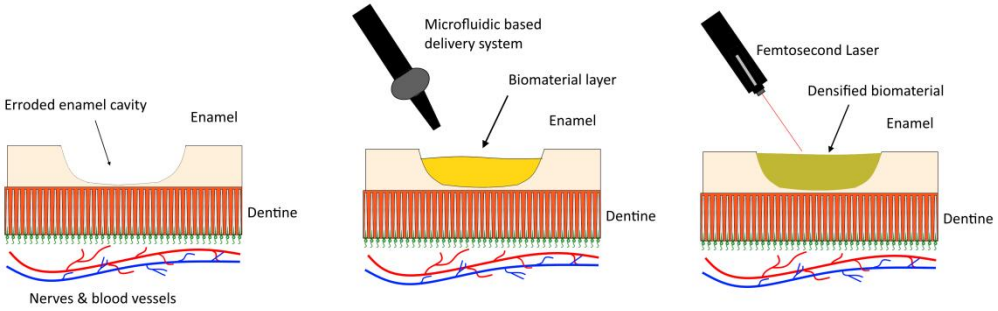


**Figure 1**: Proposed method for enamel restoration (magnified schematic cross section of exposed dentin tubules). First an eroded enamel cavity is identified, then filled with a new biomaterial which is subsequently laser irradiated to densify and bond the new material to the existing tooth.

Our first experimental results to support the feasibility of the aforementioned procedure were reported by Elmadani et al. (2012). In that work we demonstrated the sintering of erbium doped brushite crystals (DCPD: $CaHPO_4 \cdot 2H_2O$) on exposed dentine surfaces of human molars, with the use of a femtosecond laser operating at 2.5 GHz and a wavelength of 1520 nm. Brushite was considered as a suitable biomaterial because of its platelet – like crystal habit which can provide large occlusion areas while minimising heat accumulation. More recently we have confirmed that after sintering with a femtosecond laser, brushite transforms into β-pyrophosphate (BPP: $\beta\text{-}Ca_2P_2O_7$), which is the dominant phase in the irradiated area (Anastasiou et al., 2016). The localised temperature rise on the surface of

the coating, facilitates this phase transformation in the ultrafast irradiation regime. These temperatures are only superficial and confined in relatively small volume. In this investigation it was also demonstrated, that the linear absorption of laser radiation is significantly enhanced at 1040 nm wavelength, for iron doped materials, and that doping with $Fe^{3+}$ shifts the sintering temperature of the synthesised calcium phosphates to lower temperature range.

The question now arises is whether iron doped β-pyrophosphate is a suitable biomaterial for enamel restoration. So far, calcium phosphate biomaterials have been found suitable for numerous applications in dentistry. Some, include coating of metallic dental implants (Lucas et al., 1993), injectable cements for the repair of small defects, materials for the construction of bone grafts (Rungsiyanont et al., 2012) or even the addition of nanoparticles to toothpastes for the occlusion of dentine tubules or for dentine/enamel remineralisation (Tschoppe et al., 2011). Among calcium phosphate materials, hydroxyapatite is the most tested and documented because of its obvious similarity to the mineral component of bone and teeth. On the other hand, there is an insignificant amount of literature concerning the use of the minerals brushite and β-pyrophosphate for potential applications in dentistry.

The aim of the present work is to evaluate iron-doped brushite and its thermal transformation to β-pyrophosphate, as potential biomaterials for acid eroded enamel restoration. In order to establish the suitability of β-pyrophosphate for dental applications we have investigated the mechanical properties of the aforementioned biomaterials, the wear rate during brushing trials and their *in vitro* cytocompatibility with oral fibroblast cells. In order to evaluate our results we also compare the performance of our materials with dental enamel, dentine and a commercially available composite material, (Spectrum®).

## 2. Materials and methods

### 2.1. Materials synthesis

Brushite powder (Ca:P ratio 1:1) was produced following the synthesis procedure described by Elmadani et al., (2012). 200 mL of a 0.1 M $Ca(NO_3)_2{\cdot}4H_2O$ (*Fisher Chemicals, CAS:13477-34-4*) aqueous solution was heated to 37 ˚C, then a 0.1 M $(NH_4)_3PO_4$ (*Acros Organics, CAS:7783-28-0*) solution (200 mL) was added drop by drop. The final mixture was left under continuous stirring at 37 ˚C for 2 h. The solution was left to settle for 1 h to allow precipitation. The brushite crystals which formed were collected on a filter paper (Whatman grade 44 with pores of 1 µm), washed several times with distilled water and dried for 24 h at 75 ˚C. Synthesis of the $Fe^{3+}$ doped brushite (DCPD-Fe) followed a similar route, however before the addition of the $(NH_4)_3PO_4$ solution, 10% mole $Fe(NO_3)_3{\cdot}9H_2O$ (*Sigma Aldrich, CAS:7782-61-8*) was added into the calcium nitrate solution. β-pyrophosphate in powder form was needed for the particle toxicity experiments and it is known in literature that β-pyrophosphate can be obtained by thermal treatment of brushite crystals (Webb, 1966). Thus, both the undoped and the $Fe^{3+}$ doped materials, were thermally treated at 1000 ˚C for 5h in air atmosphere. The materials synthesized in this work are presented in **Table 1**.

**Table 1**: Types of materials synthesized and their identity.

| ***Name*** | ***Doping*** | ***Mineral*** |
|---|---|---|
| **DCPD-UN** | - | Un-doped brushite |
| **DCPD-Fe** | 10% Fe | 10% iron doped brushite |
| **BPP-UN** | - | Un-doped β-pyrophosphate |
| **BPP-Fe** | 10% Fe | 10% iron doped βpyrophosphate |

To test the optical and mechanical properties of the powder materials, pellets were pressed in a 13 mm diameter die. For each pellet approximately 0.25 g of the corresponding powder was filled inside the die before pressing with a load of 7 ton for 30 min, resulting thicknesses between 1 and 1.5 mm. For the β-pyrophosphate samples, pellets of brushite were heated

at 1000 ˚C for 5 h. Heat treatment resulted in the transformation of the material and densification of the pellets.

A set of bovine enamels were prepared by cutting the blocks of enamel approximately 2 mm in diameter and embedding them in epoxy resin before grinding the enamel surface flat using wet/dry paper. The flatness of the block was then characterised using non-contact profilometry (ProScan) until an RA maximum of 1.0 µm was achieved. Dental composite (Spectrum®) was pressed into a silicon mold (7 mm diameter and 1 mm thickness) and cured for 30 s in blue clinical light. The composite block was then ground flat and tested for flatness using profilometry.

**2.2. Characterisation Methods**

The crystal phase and the purity of synthesized minerals were analysed by X-Ray powder diffraction using a Philips X'Pert MPD, with monochromatic Cu K$\alpha$ radiation (0.154098 nm). For powder diffraction, a step size of 0.065° and a 2θ scanning range from 10° to 60°, was used at a scan speed of 0.014132° $s^{-1}$ to yield a powder diffraction pattern.

Scanning electron microscopy (SEM, a Hitachi SU8230 1-30 kV cold field emission gun) was used to investigate the size and shape of the powder crystals and for the identification of physical and chemical changes induced by laser irradiation. Since calcium phosphate minerals have poor electrical conductivity, prior to SEM analysis it was necessary to coat each sample with a 5 nm thick layer of platinum and then vacuum cleaning for 10 min (Quorom Technologies sputter coater and vacuum cleaner), so that the electrostatic charging during SEM analysis can be minimised.

A Simultaneous Thermal Analyser (PerkinElmer®, STA 8000) with the capability of acquiring thermogravimetric analysis (TGA) and differential thermal analysis (DTA) was employed to

investigate the chemical changes (reactions and phase transformations) which take place during the heating of the materials. All thermal experiments were carried out over a temperature range from 40 to 1500 ˚C and at a heating rate of 20 ˚C per min.

A UV-VIS spectrometer (PerkinElmer®, LAMBDA 950) equipped with a 60 mm integrating sphere module was used to measure the reflectivity of the materials. Measurements were performed on the non-irradiated pressed pellets for wavelengths between 250 and 2000 nm.

The pressed and sintered pellets were polished to ensure a flat smooth surface using 2000 grit wet/dry paper followed by polishing with a paste of 5 µm aluminium hydroxide powder. The hardness of the pellet was them measured using a microhardness tester (Sturers Duramin) with a Knoop diamond and a 100 g load for 15 s. Each pellet was tested 5 times and an average value was then taken by defining the range of variation.

The enamel, composite and sintered pellets were coated in two layers of nail varnish leaving a central strip of material exposed. The samples (pellets and enamel) were immersed under static conditions for 2 minutes five times daily in citric acid 0.3% (pH 3.2), the remaining time the samples were kept in artificial saliva ($CaCO_3$ 0.7 mM, $MgCO_3$ 0.4 mM, $KH_2PO_4$ 4 mM, KCl 31.4 mM, HEPES 20 mM) at 37 $^0$C and pH=6.8, with a minimum of one hour between each exposure to acid. Overnight the samples were immersed in a storage solution ($CaCO_3$ 0.5 mM, $MgCO_3$ 0.4 mM, $KH_2PO_4$ 0.5 mM, KCl 31.4 mM, HEPES 20 mM). The brushing trials followed the aforementioned daily cycle with the addition of two brushing steps (one at the beginning of the cycle and one before the storage of the samples). The duration of each step was 2 min (13 strokes), the mechanical load was 250 g while, a toothbrush of medium hardness was used. After 7, 14 and 21 days of the cycling regime the

depth of erosion was measured against the varnish protected areas using noncontact surface profilometry (Scatron®).

### 2.3 Cytotoxicity and genotoxicity testing

#### 2.3.1. Cytotoxicity: MTT assay

Normal oral fibroblasts were cultured in 12ml of complete Dulbecco's Modified Eagle Medium (DMEM; Sigma) in 75cm$^2$ culture flasks (Fisher) at 37$^o$C, 5% (v/v) $CO_2$. Complete DMEM consisted of high glucose DMEM supplemented with 10% (v/v) foetal calf serum (FCS), 1% (v/v) penicillin/streptomycin solution (10000 units penicillin and 10 mg streptomycin/ml; Sigma). These cells were routinely split every three days at a ratio of 1:8. To achieve this, cells were washed twice with Dulbecco's phosphate-buffered saline (DPBS) to remove all traces of serum before adding 1ml of 1X Trypsin (Sigma) to each flask. Cell were then incubated at 37 $^o$C for 2 to 3 min approximately. Once the trypsinisation process was completed, DMEM containing serum was added to the cell suspension to inhibit further tryptic activity which may damage cells. Following this, cells were pelleted, re-suspended in complete DMEM and transferred to new 75 cm$^2$ culture flasks.

Effects of the brushite and β-pyrophosphate on the viability of normal oral fibroblasts were evaluated using the MTT assay (thiazolyl blue tetrazolium bromide. Cells were seeded in 96-well plates (Fisher) at a density of 10,000 cells/well in DMEM with 10% (v/v) foetal calf serum (FCS), 1% (v/v) penicillin/streptomycin solution (10000 units penicillin and 10 mg streptomycin/ml; Sigma) and allowed to attach overnight at 37 °C with 5% $CO_2$.

After removing the culture medium by two washes with phosphate buffered saline (PBS), the toxicity assay was started with 200 µl serum-free DMEM with either undoped or iron doped materials (0–1000 µg/ml) for 24 hours. The MTT assay was performed according to the manufacturer's protocol (Sigma). Optical absorbance was read using a Labsystems iEMS

Reader MF at 540 nm. Experiments were carried out three times independently for each material. The results are expressed as mean percentage viability (±SEM) compared with untreated controls (analysed by ANOVA).

**2.3.2. Genotoxicity**

Normal oral fibroblasts (cultured as described in section 2.3.1) were plated at a density of 100,000 cells/well in 24-well plates (*Fisher*) in DMEM with 10% (v/v) foetal calf serum (FCS), 1% (v/v) penicillin/streptomycin solution (10000 units penicillin and 10 mg streptomycin/mL; Sigma) and allowed to attach overnight at 37 °C with 5% $CO_2$. After removing the culture medium by two washes with PBS, cells were incubated with 0–1000 µg/ml of either un-doped or iron doped materials in serum free DMEM for 24 h at 37 °C with 5% $CO_2$. The cells were pelleted by centrifugation at 1000 rpm for 5 min and resuspended in serum-free DMEM. A 100 µl aliquot of this suspension was mixed with 200 µl of 1% (w/v) low-melting-point agarose in PBS solution and kept at 37 °C until use. 100 µl was placed onto duplicate microscope slides (Thermo Scientific) pre-coated with 1% (w/v) agarose and covered with a coverslip (Scientific Laboratory Supplies Ltd.). Slides were placed on ice for no more than 20 s to allow the agarose to gel, after which the coverslips were removed. The slides were treated with a detergent lysis solution (2.5 M NaCl, 1 mM EDTA, 10 mM Tris, 10% DMSO, 1% Triton X-100 at pH 10) for 1 hour and placed in running buffer (300 mM NaOH, 1 mM EDTA at pH 13) at 4°C for 40 min to allow DNA unwinding, followed by electrophoresis at a constant voltage of 23 V for 20 min. Slides were finally removed, neutralised by adding 400 mM Tris at pH 7.5 for 5 min, gently dried and stained with 30 µL ethidium bromide (25 µg/ml). The stained slides were stored in damp conditions at 4°C and scored within 2 days. The slides were viewed using an Olympus BX41 microscope and digitally analysed using Komet 5.5 software. Cells were scored by evaluating 50 cells per

slide, with duplicate slides for every sample. Experiments were carried out three times independently for each of the materials. The results are expressed as mean percentage tail DNA (±SEM, analysed by ANOVA). 0 μg/ml represents the negative controls.

**2.3.3. Cell preparation for transmission electron microscopy (TEM) imaging**

Normal oral fibroblasts (cultured as described in section 2.3.1) were plated at a density of 100,000 cells/well in 24-well plates (Fisher) in DMEM with 10% (v/v) foetal calf serum (FCS), 1% (v/v) penicillin/streptomycin solution (10000 units penicillin and 10 mg streptomycin/ml; Sigma) and allowed to attach overnight at 37 °C with 5% $CO_2$.

Following seeding of the cells, culture medium was removed and cells washed twice with PBS. Cells were then incubated with 0–1000 μg/ml of either undoped or iron doped materials in serum free DMEM for 24 h at 37°C with 5% $CO_2$. Cells were then pelleted, washed with pre-warmed PBS and fixed with 100 mM phosphate buffered with 2.5% EM grade Glutaraldehyde for 15 min at 37 ˚C. Cells were pelleted, fixative was removed, pellet resuspended and fresh 2.5% Glutaraldehyde added. Cells were incubated at 4 $^{o}$C for 4 hours to allow the fixation process to take place. Cells were then pelleted, washed with fresh maintenance solution and resuspended. To post fix, 1% osmium tetroxide fixative was added (Millonigs 100mM phosphate buffer, pH 7.3) and incubated for 1.5 h in the dark at room temperature. Cells were once again pelleted and from this step onwards, each solution was pipetted on and aspirated off, being careful not to resuspend the cell pellet. Four dehydration steps were carried out: 10% ethanol for 10 min; 50% ethanol for 15 min; 70% ethanol for 15 min; and 100% ethanol for 10 min. Tubes were sealed with parafilm and stored at 4 ˚C overnight.

In order to embed the cells in resin (Agar Araldite CY212 Epoxy), each sample was washed with propylene oxide twice for 20 min, then incubated in propylene oxide and araldite (1:1)

for 16 h, followed by transfer to propylene oxide and araldite (1:3) for several hours and finally transferred into pure araldite for 8 h. The cells were transferred to embedding moulds containing fresh araldite, which was then polymerised for 16 h at 60 °C. Ultrathin sections of 80-100 nm thickness were cut using an ultramicrotome (Reichert-Jung, Ultracut-E) with a diamond knife. Sections were then mounted on continuous carbon support grids (Agar Scientific Ltd), sputtered coated with ~ 10 nm of amorphous carbon (Quorum Technologies coater) and imaged using a Tecnai F20 FEG-TEM operated at 200 kV and fitted with a Gatan Orius CCD camera and Oxford Instruments 80 $mm^2$ Xmax SD X-ray detector running Aztec processing software.

## 3. Results

### 3.1. Characterisation of the synthesised materials

X-Ray diffraction patterns for the initial, laser irradiated and heat treated materials are presented in **Fig 2** for the DCPD-UN (**Fig. 2a**) and the DCPD-Fe (**Fig. 2b**) brushite. The purpose of this comparison is to demonstrate that the changes arisen to the mineral after irradiation with a femtosecond laser (with the parameters described in Anastasiou et al., (2016)) are comparable with the mineral after thermal treatment for 5 h at 1000 ˚C. The starting material is identified as pure brushite since all the significant peaks coincide with the peaks of the reference pattern JCPDS-01-074-6549 (• for brushite). After laser irradiation is β-pyrophosphate which dominates at the surface of the samples (as discussed in Anastasiou et al., 2016). The majority of the peaks are assigned to the β-pyrophosphate reference pattern (JCPDS-04-009-8733; □ for β-pyrophosphate), except the residual brushite (0 2 0) and (0 4 0) peaks which are still present at 2θ=11.56˚ and 23.51˚, respectively. Given that the penetration depth of the X-ray beam ranges from 20 to 120 μm (depending on the Bragg angle, 2θ) and that the depth of transformation due to laser energy has been shown

to be between 40-60 μm (Anastasiou et al., 2016), it is likely that while there is complete transformation of the material at the surface of the pellet, the underlying mineral might remain unaltered (i.e. brushite). As it is evident from the X-Ray diffraction patterns, heat treatment of brushite at 1000 ˚C results into a complete transformation of the mineral to β-pyrophosphate (all peaks have been assigned to the JCPDS-04-009-8733 reference pattern) and all the peaks match with those found for the laser irradiated materials (except the two residual brushite peaks identified in the laser irradiated samples).

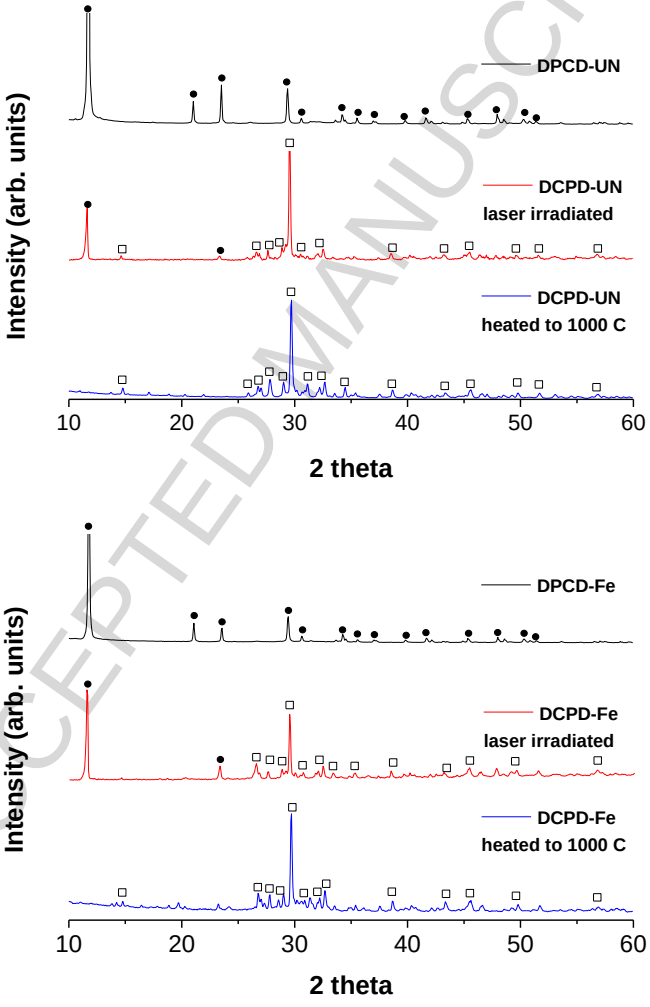


**Figure 2**: X-Ray diffraction patterns for the starting, irradiated and heated powders; a) for the undoped (DCPD-UN) material; b) for the 10% Fe-doped (DCPD-Fe) material. Brushite and β-pyrophosphate reflections are labelled with • and □ respectively. Only the major peaks of these two phases are labelled.

SEM images of the initial, heat treated and laser irradiated materials are presented in **Fig. 3** for the un-doped and $Fe^{3+}$ doped samples. From **Fig. 3a** and **Fig. 3b** it is evident that the

original brushite crystals for both minerals have comparable morphology. Comparing the heated un-doped brushite (**Fig. 3c**) with heated $Fe^{3+}$ doped brushite (**Fig. 3d**), it is apparent that both have transformed morphology (to β-calcium pyrophosphate; **Fig 2**). However, outlines of the original brushite platelets (now porous) are still present in the images of the heat treated un-doped powder (**Fig. 3c**). On the other hand, the doped material has transformed and partially densified without the formation of significant surface pores. Similarly to these findings the laser irradiated DCPD-UN pellet surface retains the original brushite crystal forms however, micro-porosity and micro cracks are present due to water removal during the brushite to pyrophosphate transformation (**Fig 3e** and as discussed in Anastasiou et al., 2016). At the same time the laser irradiated DCPD-Fe pellet (**Fig. 3d**) has sintered and remineralised without the formation of micropores and significantly lower cracking, similarly to the heated DCPD-Fe powders (**Fig 3d**).

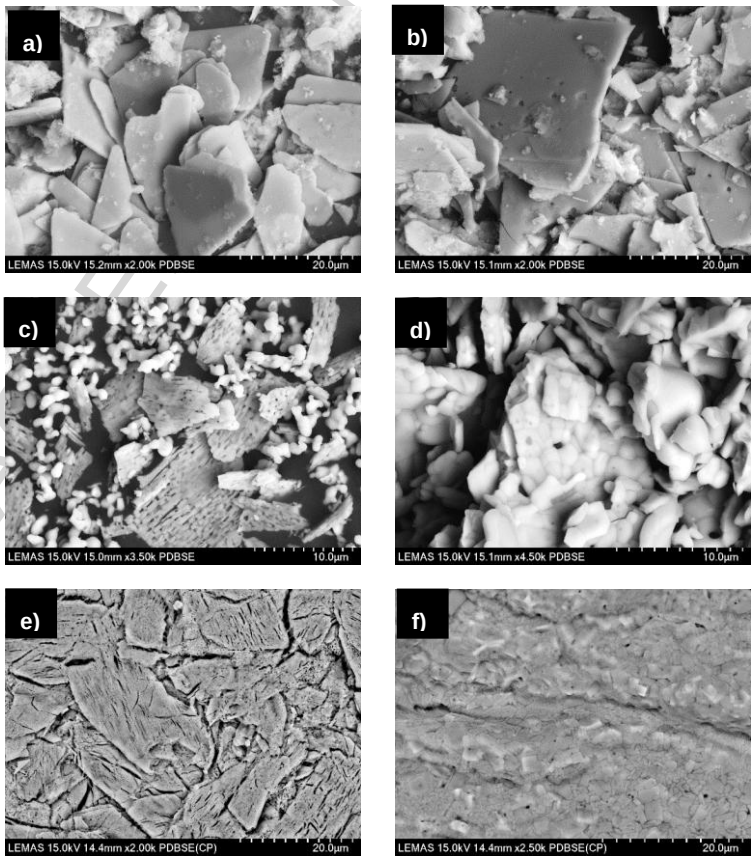

**Figure 3**: SEM images of the initial and the heated materials; a) initial un-doped brushite crystals; b) initial Fe-doped brushite crystals; c) un-doped brushite powder heated at 1000 C exhibiting transformation with retention of some original plates containing considerable microporosity ; d) Fe-doped brushite powder heated at 1000 C exhibiting both morphology transformation and some densification without significant surface microporosity; e) surface image of the laser irradiated un-doped brushite pellet showing microporosity and cracks on the relics of the original powder morphology; f) surface image of the laser irradiated Fe-doped brushite pellet showing densification without large-scale microporosity or cracks.

The different behaviour upon heating (and laser irradiation) of the doped and un-doped materials can be attributed to the phase transformation temperatures of each one of these materials. The transformation of pure brushite to β-pyrophosphate takes place at 813 ˚C (Anastasiou et al., 2016) and with further heating to 1293 ˚C, the β form changes to α-$Ca_2P_2O_7$ which is not very stable and in many cases transforms back to the β form during cooling (Bian et al., 2004). The melting point is identified at 1380 ˚C. These transformation peaks are shifted to lower temperatures for the $Fe^{3+}$ doped material as shown in **Fig. 4**. Specifically, the β to α-$Ca_2P_2O_7$ transformation now occurs at 1012 ˚C, the melting point has been reduced to 1272 ˚C while, during cooling the α to β-$Ca_2P_2O_7$ transformation takes place at 855 ˚C. From these results it is easy to understand that although after heat treatment at 1000 ˚C the final product of the two materials (Fe-DCPD and DCPD) is the same (β-pyrophosphate as it was identified by X-ray diffraction in **Fig. 4**) the pathway to this is different for each case.

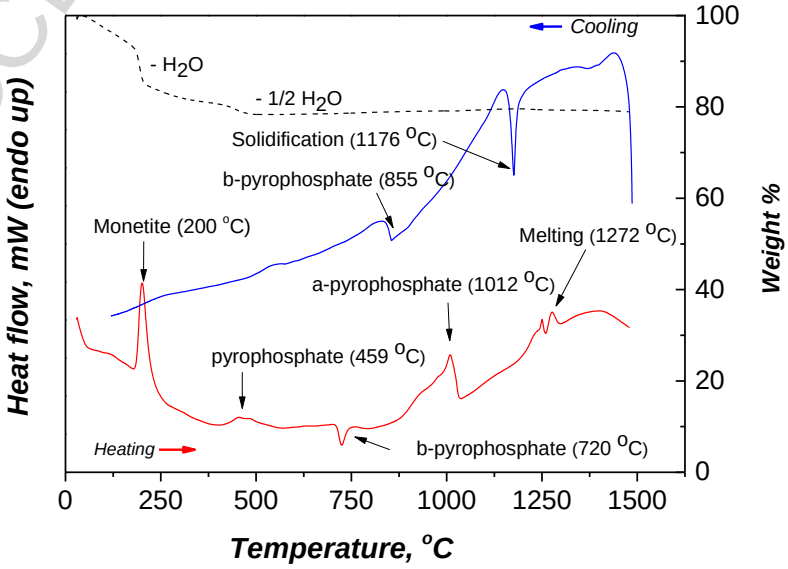

**Figure 4***:* Thermal analysis of iron doped brushite (DPCD-Fe) and identification of the phase transformation temperatures for heating/cooling rate of 20 ˚C/min (the DSC curve is shown in red for heating and blue for cooling and values reported on the LH y-axis while the TGA curve is shown with the dashed line and values reported on the RH y-axis). The key transformation temperatures are marked.

Optical reflectivity measurements for the DCPD-UN, DCPD-Fe samples and dental enamel are presented in **Fig. 5**. As expected, doping with $Fe^{3+}$-ions increases photon optical absorption of brushite in the 800 -1050 nm regime. At the 1040 nm fs-pulsed laser irradiation wavelength, reflectivity for un-doped brushite is 83%, which drops to around 72% for $Fe^{3+}$-doped brushite while, reflectivity of dental enamel for the same wavelength is 86%.

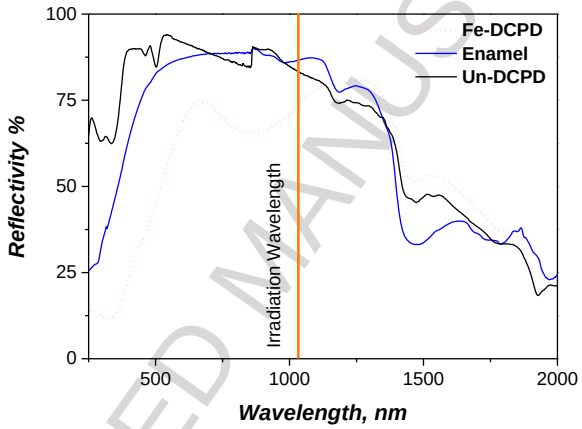


**Figure 5:** Reflectivity measurements for brushite (DCPD-UN), $Fe^{3+}$-doped brushite (DCPD-Fe) and dental enamel show that $Fe^{3+}$ doping increases the absorption at 1045 nm wavelength.

### 3.2. Mechanical properties and brushing trials

The hardnesses of the undoped pyrophosphate (BPP-Un) and Fe doped (BPP-Fe) pyrophosphate pellets are presented and compared with the hardnesses of natural enamel, dentine and a commercial composite polymer in **Fig 6**. The hardness of the iron doped pellet is significantly higher than that of the undoped pellet (265 HK for BBP-Fe and 32.5 HK for BBP-Un), is similar to that of natural enamel (298 HK) and is much harder than the currently available restorative materials (hardness of the composite is 33 HK).

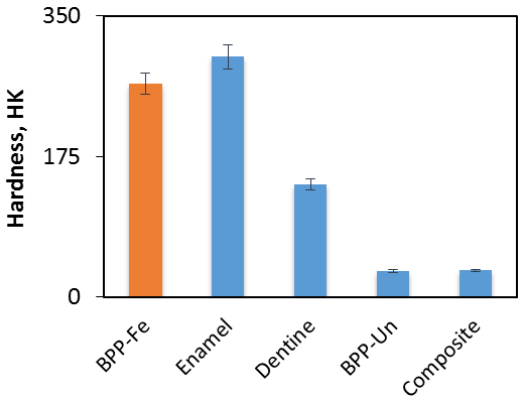


**Figure 6:** Hardness of iron-doped (BBP-Fe) and un-doped (BPP-Un) β-pyrophosphate thermally sintered pellets and comparison with enamel, dentine and a commercial composite material (Spectrum ®).

Before the simulated tooth brushing trials all pellets were tested for mass loss when immersed in the citric acid solution over a two week pH cycle without applying any mechanical load. The DCPD-UN, DCPD-Fe and BPP-Un pellets fell apart after 3 days whereas, the BPP-Fe pellet remained intact over the full cycle. For this reason BPP-Fe was the only material tested during the extended brushing trials.

The results of the 3 week simulated tooth brushing trials are presented in **Fig. 7**. The depth of erosion for the natural enamel is measured to be around 4 µm after the first week of the testing, increasing to 12 µm after the second week and reaches 17.54 µm at the end of the third (**Fig. 7a**). The enamel sample show significant erosion and mass loss in both SEM and profilometry images of the brushed surface (**Fig 7b** and **Fig. 7d** respectively). On the other hand limited erosion (0.6 µm) can be detected on the surface of the BPP-Fe pellet (**Fig. 7a**). After SEM imaging (**Fig. 7b and Fig. 7c**) and profilometry scanning (**Fig. 7e**) we were able to identify only some traces of erosion on the BPP-Fe pellet.

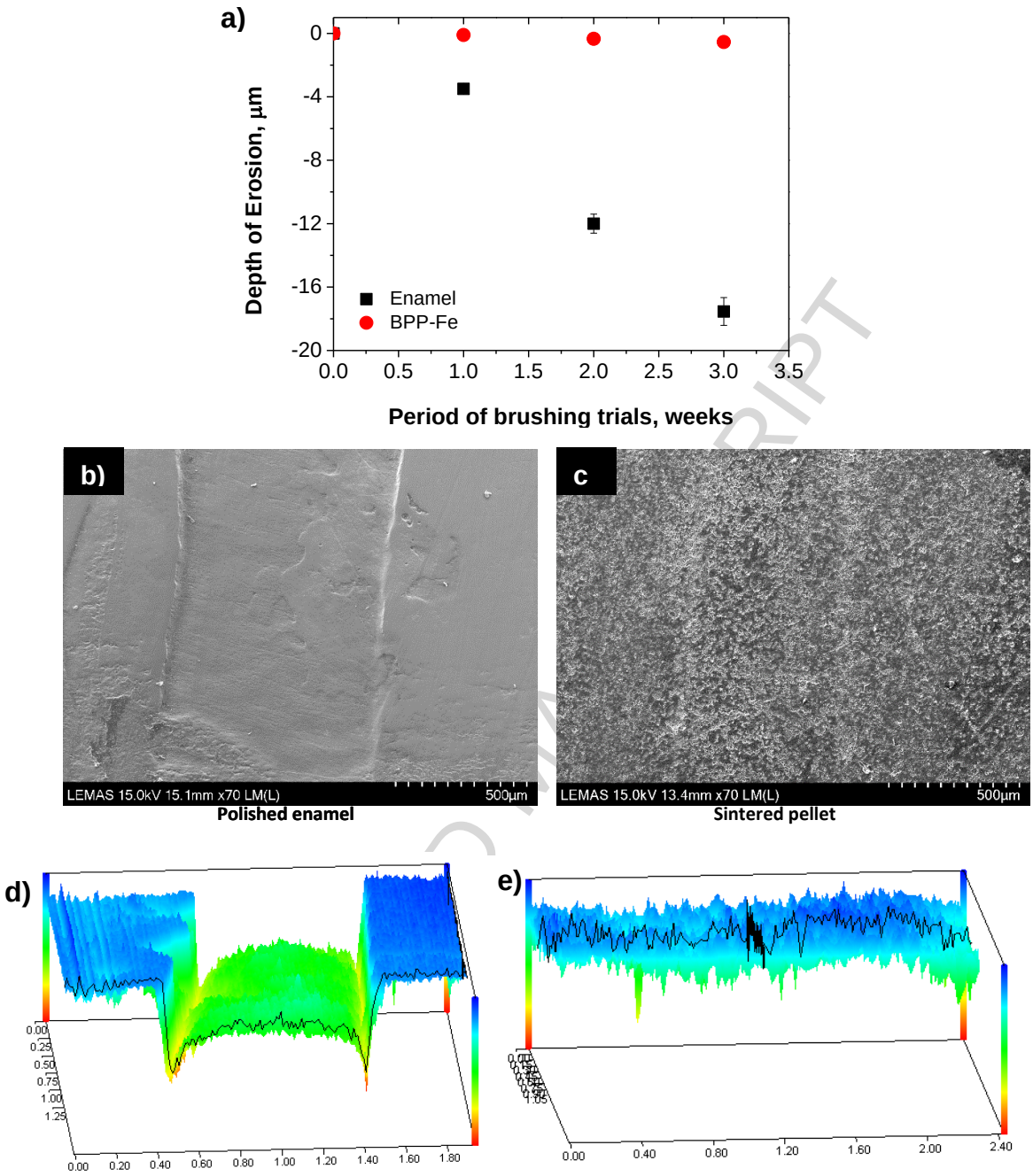


**Figure 7:** Comparison of the measured erosion depth between natural enamel and an Fe-doped β-pyrophosphate pellet after a three week simulated tooth brushing trial; a) erosion during three weeks of brushing trials (error bars of 5% represent the maximum deviation between the three replicates of each sample); b) SEM image of dental enamel after the second week of the trial showing a clearly eroded brushing track; c) SEM image of BPP-Fe pellet after the second week of the trial showing no significant erosion along the brushing track; d) profilometry of dental enamel at the end of the second week of the trial indicating the depth of materials loss ; e) proflilometry of the BPP-Fe pellet at the same time point indicating minimal material loss .

### 3.3. Cytotoxicity and genotoxicity testing

In this study normal oral fibroblasts were exposed to a range of concentrations of either undoped or iron doped β-pyrophosphate particles. Potential cytotoxicity and genotoxicity

was assessed by MTT and comet assays, respectively. **Figures 8a** and **8b** show a statistically significant reduction in cell viability compared to controls only in the presence of undoped materials at exposure levels of 100 and 1000 µg/ml for undoped brushite (DCPD-Un) and from 1 µg/ml for undoped β-pyrophosphate (BPP-Un). No DNA damage was detected by the comet assay in any samples as shown in **Fig. 9a** and **9b**.

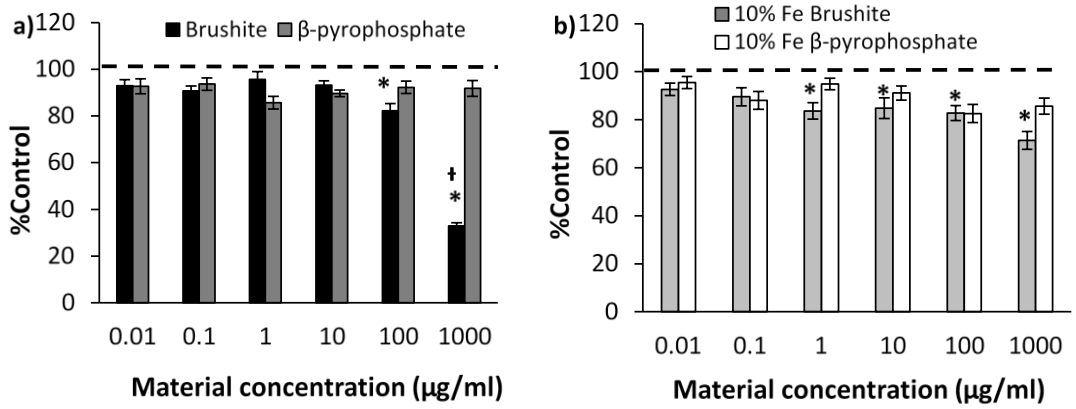


**Figure 8:** Cell viability (by MTT assay) measured in normal oral fibroblasts at 24 h of treatment with; a) undoped materials (brushite and b-pyrophashate); b) iron doped materials. Results are percentage values (Mean ± SEM) where 100% corresponds to control values (untreated cells). *Significantly different from control values ($p<0.05$) by one-way ANOVA followed by Dunnett's multiple comparison test. ǂSignificantly different from β-pyrophosphate values ($p<0.05$) by 2 sample t-test. Significant responses are seen at 100 and 1000 µg/mL and above 1 µg/mL for undoped and iron doped brushite respectively.

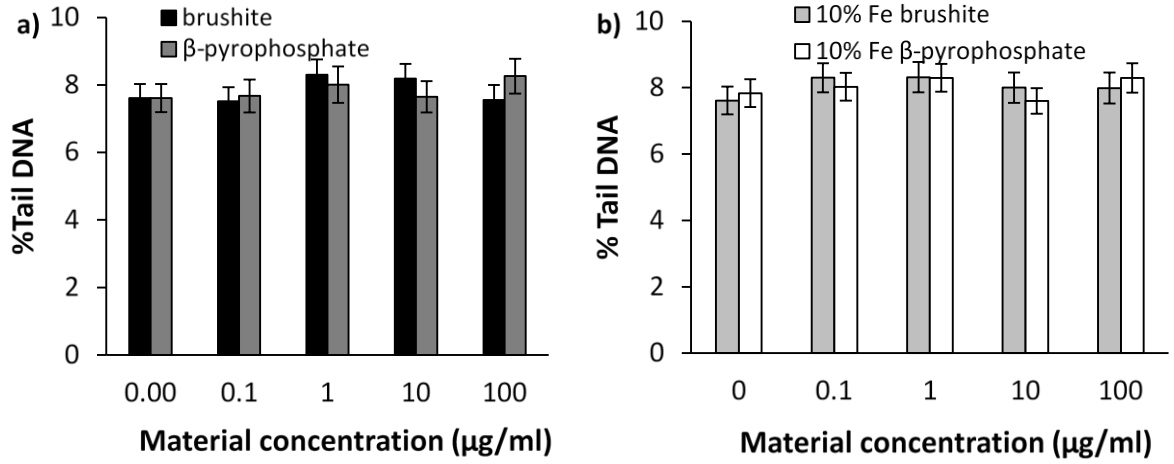


**Figure 9:** Genotoxicity (by comet assay) measured in normal oral fibroblasts at 24 h of treatment with; a) undoped materials; b) iron doped materials. Results are percentage values (Mean ± SEM). No significant responses are observed at any exposure levels tested.

### 3.4. Particle uptake by the fibroblast cells

Transmission electron microscopy imaging was carried out in order to assess whether normal oral fibroblasts do uptake brushite or β-pyrophosphate particles or particle

fragments (100 µg/ml). Evidence of cellular uptake of these particles is shown in **Fig. 10**. Clearly, particle fragments are taken up without significant impact on the cellular ultrastructure. The calcium phosphate nature of the particles was confirmed by spot Energy Dispersive X-ray EDX (**Fig. 10**).

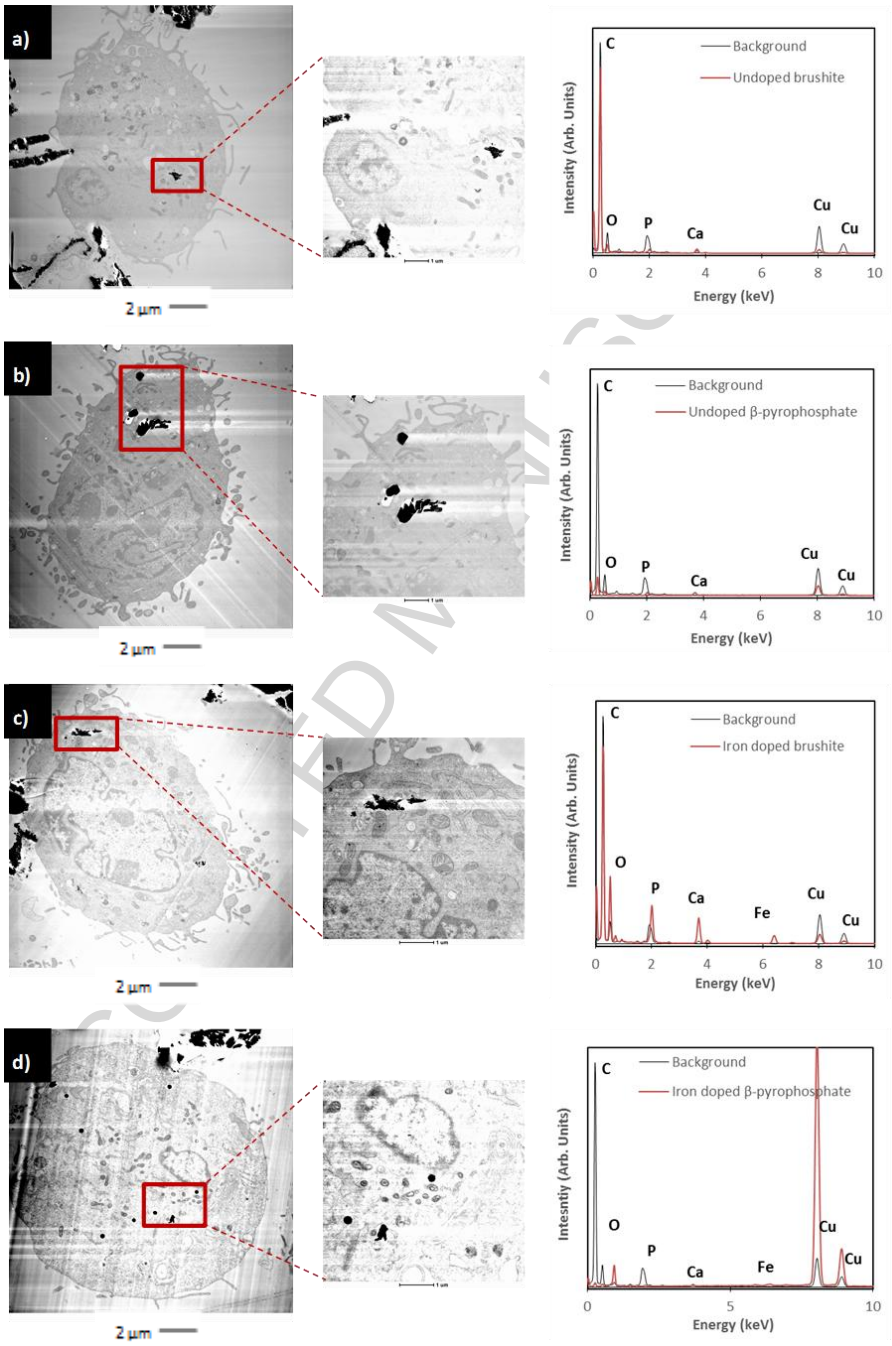


**Figure 10:** TEM imaging and analysis of normal oral fibroblasts treated with calcium phosphate materials; Contrast-inverted scanning TEM image of a cell followed by higher magnification image and EDX spectrum from the area indicated a) Undoped brushite; b) Undoped β-pyrophosphate; c) Iron doped brushite; d) Iron doped β-pyrophosphate.

## 4. Discussion

Although sintering of un-doped (DCPD-UN) and 10% Fe-doped (DCPD-Fe) brushite to 1000 ˚C results in both cases in the transformation to β-pyrophosphate (**Fig. 11**) the micro-structure and the mechanical properties of the two materials are completely different. When the DPCD-UN sample is heated to 1000 ˚C the γ- $Ca_2P_2O_7$ transforms to β- $Ca_2P_2O_7$ at 813 ˚C and this is the final product of the heat treatment. On the other hand, when the DCPD-Fe sample is heated at 1000 ˚C the γ- to β- transformation takes place at 720 ˚C and at 1000 ˚C the formation of the unstable α-pyrophosphate occurs (the transformation peak has been identified at 1012 ˚C but as presented in **Fig. 4** the process begins below 1000 ˚C). The latter phase transforms back to β-$Ca_2P_2O_7$ during cooling at a temperature of 833 ˚C. Thus although the final product after heating is the same for the DCPD-Un and Fe materials, the extra two transformation steps observed at 1000 ˚C for the DCPD-Fe result in its total remineralisation to a different particle morphology and even produces particle sintering and densification. These results are consistent with the reported transformations of the two materials after laser irradiation (Anastasiou et al., 2016). The only difference between heat treatment and laser irradiation is that in the first case the transformations occur in the bulk of the material while in the second case we have only alterations of the surface (up to 40-60 μm deep).

The benefits of doping with iron are not restricted only to the enhancement of the sintering process. Iron increases the optical absorption of the minerals at 1040 nm wavelength in comparison to the absorption of dental enamel (**Fig 6**). This is crucial for the proposed laser treatment procedure since any thermal damage to the underlying hard tissues would be minimised. Generally, the energy absorption rate which transforms to heat (S) during the

irradiation of the samples is a function of the laser energy fluence (J), the pulse duration ($t_p$), the radiation penetration depth (δ) and the material's reflectivity (R) (**eq. 1**) (Tzou and Chiu, 2001). If we expose DCPD-Fe and dental enamel to the same laser beam (with fixed J, $t_p$ and δ) reflectivity is the only parameter that differs. Utilising **eq. 1** for the two cases it can be shown that the energy absorption rate is 2 times higher for the DCPD-Fe, leading to higher surface temperatures than for enamel and this way we can control and minimise any thermal damage induced to the tooth.

$$S = 0.94\frac{(1-R)J}{t_p\delta}\exp\left(-\frac{x}{\delta}-\frac{1.992\left(t-2t_p\right)}{t_p}\right) \qquad \textbf{eq. 1}$$

The hardness of iron doped pyrophosphate pellets are found to be similar to natural enamel and much harder than un-doped pyrophosphate pellets produced with the same thermal treatment (**Fig 6**). As discussed before, sintering and densification are more pronounced by the presence of iron and that results in the significant difference in the hardness of the two materials. The great difference (order of magnitude) in the erosion depth between the enamel and the iron doped pyrophosphate can be attributed to the low solubility of pyrophosphate in comparison to natural enamel. It is known that hydroxyapatite of enamel, due to carbonate substitutions in the mineral crystal lattice, is more acid soluble and that is significant cause of enamel wear in the first place (Lussi, 2006).

Exposure of oral fibroblasts in vitro to increasing concentrations of brushite and β-pyrophosphate particles (undoped and iron doped) only proved to affect cell viability at higher concentrations of undoped materials (**Fig 8**) and did not cause DNA damage (**Fig 9**). Iron doped β-pyrophosphate produced the least response of the cells to particle exposure (despite clear evidence of particle uptake; **Fig 10**) and so could be considered the most cytocompatible of all the materials tested. In the recent work of Manchon et al. (2015), β-

tricalcium phosphate powders doped with different concentrations of iron (from 10 to 30% mol) were tested for cytocompatibility. They also report the absence of any toxic effect of iron doped ceramics on the osteoblast-like cell line MG-63. Finally, the uptake of the calcium phosphate particles or particle fragments by the cells is a normal phenomenon since it is known that fibroblasts are involved in the degradation process of minerals through phagocytic mechanisms (Sheikh et al., 2015).

Overall, this work demonstrates the suitability of the iron doped minerals for the restoration of dental enamel through the procedure described in **Fig. 1**. Moreover, in recent experiments we observed that iron doped material (DCPD-Fe) can be successfully laser sintered on enamel surface (**Fig. 11**). After irradiation with a 1 GHz femtosecond laser (1040 nm wavelength and average power of 0.4 W) the produced BPP-Fe layer is strongly attached on dental enamel while in some cases the interface between enamel and the new biomaterial is hard to be distinguished (**Fig. 11**).

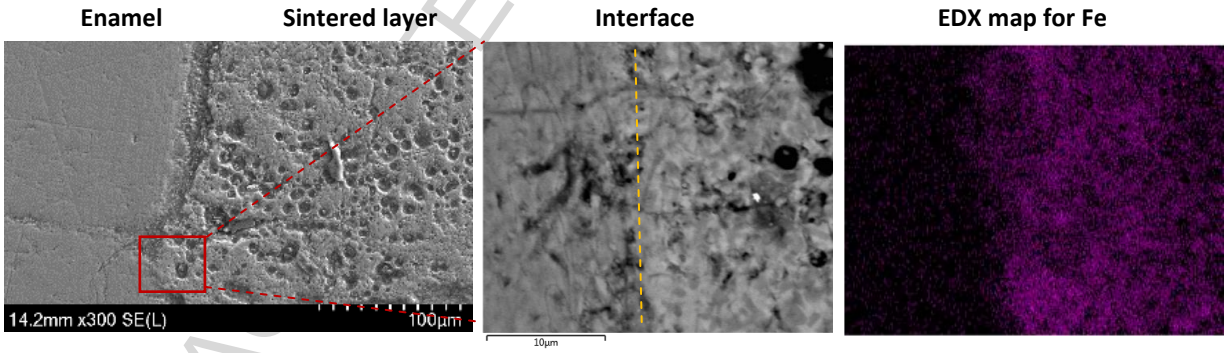


**Figure 11**: Sintered Fe-doped pyrophosphate on enamel surface, magnified image of the interface and EDX map for identifying Fe. Experiments have been conducted with 1 GHz femtosecond laser, emitting at 1040 nm. The irradiation parameters are the same as described in Anastasiou et. al., (2016).

## 5. Conclusions

The aim of this work was the evaluation of iron doped β-pyrophosphate as a potential biomaterial for dental applications and specifically for the restoration of dental enamel. The mechanical properties and cytocompatibility of this material were tested and compared to

the properties of dental enamel, dentine and a commercial composite for enamel restoration. The most important outcomes of this research could be concluded as the following:

- We demonstrate that doping brushite with 10 mol% iron ($Fe^{3+}$), can improve thermal and laser sintering at 1000 $^{o}$C.
- Iron doped β-pyrophosphate pellets sintered at 1000 ˚C have the same hardness as natural enamel and are considerably harder than dentine and a commercial restorative material (composite).
- We show that iron doped β-pyrophosphate pellets sintered at 1000 $^{o}$C can perform better than natural enamel during simulated tooth-brushing trials s. There were no signs of erosion or mass loss on the tested iron doped β-pyrophosphate pellet. This is attributed to the higher stability of the pyrophosphate when exposed to pHs lower than 5.
- Cytotoxicity and genotoxicity testing suggest that iron doped β-pyrophosphate is cytocompatible and therefore could be used in dental applications.

With the results of this work we demonstrate that β-pyrophosphate is a promising material for dental applications and specifically for enamel restoration. Its stability at low pH and the slow wear rate indicate that it can restore and even enhance natural enamel. Going forward we will next assess the strength and integrity of a β-pyrophosphate layer laser irradiated onto enamel.

**Acknowledgments**

The authors acknowledge support from the sponsors of this work; the EPSRC LUMIN (EP/K020234/1) and EU-Marie-Curie-IAPP LUSTRE (324538) projects. Also authors would like to acknowledge Dr Helen Colley for supplying the oral fibroblast cell lines, Mr. Mohammed Javed for the laboratory support and Mr. John Harrington and Mr. Stuart Micklethwaite for SEM support.

## References


ANASTASIOU, A. D., THOMSON, C. L., HUSSAIN, S. A., EDWARDS, T. J., STRAFFORD, S., MALINOWSKI, M., MATHIESON, R., BROWN, C. T. A., BROWN, A. P., DUGGAL, M. S. & JHA, A. 2016. Sintering of calcium phosphates with a femtosecond pulsed laser for hard tissue engineering. *Materials & Design*.

BIAN, J.-J., KIM, D.-W. & HONG, K.-S. 2004. Phase transformation and sintering behavior of $Ca_2P_2O_7$. *Materials Letters,* 58**,** 347-351.

CROISIER, F. & JÉRÔME, C. 2013. Chitosan-based biomaterials for tissue engineering. *European Polymer Journal,* 49**,** 780-792.

ELMADANI, E., JHA, A., PERALI, T., JAPPY, C., WALSH, D., LEBURN, C., BROWN, T., SIBBETT, W., DUGGAL, M. & TOUMBA, J. 2012. Characterization of Rare-Earth Oxide Photoactivated Calcium Phosphate Minerals for Resurfacing Teeth. *Journal of the American Ceramic Society,* 95**,** 2716-2724.

KLEVERLAAN, C. J. & FEILZER, A. J. 2005. Polymerization shrinkage and contraction stress of dental resin composites. *Dental Materials,* 21**,** 1150-1157.

LUCAS, L. C., LACEFIELD, W. R., ONG, J. L. & WHITEHEAD, R. Y. 1993. Calcium phosphate coatings for medical and dental implants. *Colloids and Surfaces A: Physicochemical and Engineering Aspects,* 77**,** 141-147.

LUSSI, A. 2006. *Dental Erosion: From Diagnosis to Therapy*, Karger.

MANCHON, A., HAMDAN ALKHRAISAT, M., RUEDA-RODRIGUEZ, C., PRADOS-FRUTOS, J. C., TORRES, J., LUCAS-APARICIO, J., EWALD, A., GBURECK, U. & LOPEZ-CABARCOS, E. 2015. A new iron calcium phosphate material to improve the osteoconductive properties of a biodegradable ceramic: a study in rabbit calvaria. *Biomed Mater,* 10**,** 055012.

MCCABE, J. F. & WALLS, A. W. G. 2013. *Applied Dental Materials*, Wiley.

PANSERI, S., CUNHA, C., D'ALESSANDRO, T., SANDRI, M., RUSSO, A., GIAVARESI, G., MARCACCI, M., HUNG, C. T. & TAMPIERI, A. 2012. Magnetic Hydroxyapatite Bone Substitutes to Enhance Tissue Regeneration: Evaluation *In Vitro* Using Osteoblast-Like Cells and *In Vivo* in a Bone Defect. *PLoS ONE,* 7**,** e38710.

RUNGSIYANONT, S., DHANESUAN, N., SWASDISON, S. & KASUGAI, S. 2012. Evaluation of biomimetic scaffold of gelatin–hydroxyapatite crosslink as a novel scaffold for tissue engineering: Biocompatibility evaluation with human PDL fibroblasts, human mesenchymal stromal cells, and primary bone cells. *Journal of Biomaterials Applications,* 27**,** 47-54.

SHEIKH, Z., ABDALLAH, M.-N., HANAFI, A.-A., MISBAHUDDIN, S., RASHID, H. & GLOGAUER, M. 2015. Mechanisms of in Vivo degradation and resorption of calcium phosphate based biomaterials. *Materials,* 8**,** 7913-7925.

SMITH, B. D. & GRANDE, D. A. 2015. The current state of scaffolds for musculoskeletal regenerative applications. *Nat Rev Rheumatol,* 11**,** 213-222.

TSCHOPPE, P., ZANDIM, D. L., MARTUS, P. & KIELBASSA, A. M. 2011. Enamel and dentine remineralization by nano-hydroxyapatite toothpastes. *Journal of Dentistry,* 39**,** 430-437.

TZOU, D. Y. & CHIU, K. S. 2001. Temperature-dependent thermal lagging in ultrafast laser heating. *International Journal of Heat and Mass Transfer,* 44**,** 1725-1734.

WEBB, N. 1966. The crystal structure of [beta]-$Ca_2P_2O_7$. *Acta Crystallographica,* 21**,** 942-948.

YAN, L., CHAI TECK, N. & CHUI PING, O. 2009. Iron(III) and manganese(II) substituted hydroxyapatite nanoparticles: Characterization and cytotoxicity analysis. *Journal of Physics: Conference Series,* 187**,** 012024.

Highlights

- A novel procedure for the restoration of dental enamel is introduced
- Iron doped β-pyrophosphate is evaluated as potential biomaterial for enamel restoration
- Iron doped β-pyrophosphate found to have the same hardness as natural enamel and dramatically lower wear rate
- Cytotoxicity and genotoxicity tests suggest that iron doped β-pyrophosphate is cytocompatible and safe for dental applications